Geoscience Letters

RESEARCH LETTER

Open Access

Unprecedented warming in Northwestern India during April of 2022: roles of local forcing and atmospheric Rossby wave

Jianhuang Qin[1,2*], Heng Liu[1] and Baosheng Li[2,3]

Abstract

A high surface air temperature (SAT) record over Northwestern India was reported in April 2022. This study examines the contribution of interannual variability on Indian SAT and possible reasons for the extreme SAT during April 2022. Result shows that the interannual variability of SAT is captured by the first two leading modes using the empirical orthogonal function (EOF) analysis. Both of them show highest values over the Northwestern India and are simultaneous energetic during 2022. The EOF1 is related to the Indian Ocean Basin Mode (IOBM) and an anomalous anti-cyclone in the troposphere, while the Rossby wave train from the North Atlantic to the north of India controls the EOF2. The active IOBM and strong Rossby wave source account for the extreme SAT over northwestern India during April 2022. In addition, the Indian regional mean SAT during April is well represented by the indices of IOBM and tropospheric anomalous anti-cyclone, which can help to improve the prediction of SAT over India.

Introduction

Indian continent is a highly populated area with a major center of agriculture, industry and economy. Under the influence of global warming, a significant increasing temperature in all the places of India is observed, accompanied by decreased annual and monsoon rainfall (Krishnan et al. 2016). The drought and heat wave extremes are becoming more and more frequent over India (Rohini et al. 2016; Pai et al. 2017), which are increasing threats to human property and health (Sanjay et al. 2020). Therefore, it is very important to investigate the drivers and processes responsible for surface air temperature (SAT) variability over India.

*Correspondence:
Jianhuang Qin
qinjianhuang@163.com
[1] College of Oceanography, Hohai University, Nanjing, China
[2] Southern Marine Science and Engineering Guangdong Laboratory (Zhuhai), Zhuhai, China
[3] State Key Laboratory of Satellite Ocean Environment Dynamics, Second Institute of Oceanography, Ministry of Natural Resources, Hangzhou, China

Most previous studies focused on the rapid rise in Indian SAT and its diurnal asymmetry (e.g., Kumar et al. 1994; Roy and Balling 2005; Rai et al. 2012; Blunden et al. 2018; Ross et al. 2018). For instance, the mean annual temperature of India has an increase with 0.4 °C/100 year during the twentieth century (Hingane et al. 1985), and the warming over India has accelerated after 1990s (Sanjay et al. 2020). Such Indian warming was solely contributed by maximum temperatures (Kothawale and Kumar 2005). Besides the trend, the Indian SAT has an annual cycle and remarkable interannual variability, which account for the high temperature extremes and heat waves. Using the empirical orthogonal function (EOF) analysis, Chowdary et al. (2014) suggested that the interannual variability of seasonal Indian SAT is characterized by the first two leading EOF modes. They further found that the country-wide warming pattern (i.e., EOF1) is linked to El Niño-Southern Oscillation (ENSO; Bjerknes 1969). However, the relationship between the Indian SAT and ENSO is not stable. Severe heat waves do not always occur after El Niño events (Kalsi and Pareek, 2001). In addition to the influences of ENSO and global warming,

the heat wave condition is related to the local anomalous circulation setting over India and its neighborhood (De et al., 2005). In all, the interannual variability of SAT over India remains an interesting issue, and has not been totally examined.

Since the pre-monsoon temperatures displayed the highest warming trend in recent years, more attention was paid into concern the extreme values of temperature before the onset of Indian summer monsoon. In observations, the long lasting heat waves over India are becoming more frequent during April–June (Rohini et al. 2016). The extreme high temperature during the pre-monsoon season causes tens of thousands of deaths in recent years. Commonly, the April mean SAT is around 30 °C with the maximum in the central India (Fig. 1a). During April 2022, the maximum temperature reached an unprecedented high value. In particular, the anomaly of daily mean SAT is larger than 5 °C over northwestern India (Fig. 1b). The SAT index (SATI) is defined as the regional mean SAT over India, which also has a high value exceeding 28.5 °C during April 2022 (Fig. 1c). Such abnormal high temperature is exacerbated by increasing trend and interannual variability of SAT over India. With the exception of the influences of global warming and ENSO, it should be considered the mechanism of interannual SAT variability over India during April and the possible reasons for the extreme SAT in 2022. This is the aim of this study. The remainder of this paper is organized as follows. Data and methods used in this study are introduced in "Data and methods" Section. In "Results" Section, the mechanism of Indian SAT during April is investigated, followed by "Conclusion and discussion" Section.

Data and methods

The atmospheric variables, including sea level pressure, SAT, multilevel geopotential heights, zonal and meridional winds, vertical velocity and specific humidity, are obtained from the European Center for Medium-Range Weather Forecast (ECMWF) ERA5 reanalysis dataset (Hersbach et al. 2019) with a horizontal resolution of 0.25 °, and the National Centers for Environmental Prediction–National Center for Atmospheric Research (NCEP–NCAR; Kalnay et al 1996) with a horizontal resolution of 2.5 °. The SSTs from version 5 of the National Oceanic and Atmospheric Administration's (NOAA's) Extended Reconstructed SST dataset (ERSST v5) are also used, which have a horizontal resolution of 2 °. The regional mean SATI has an increasing trend obtained from two reanalysis (Fig. 1c). The trend is 0.0167 °C/year calculated by the ERA5, and 0.0069 °C/year obtained from

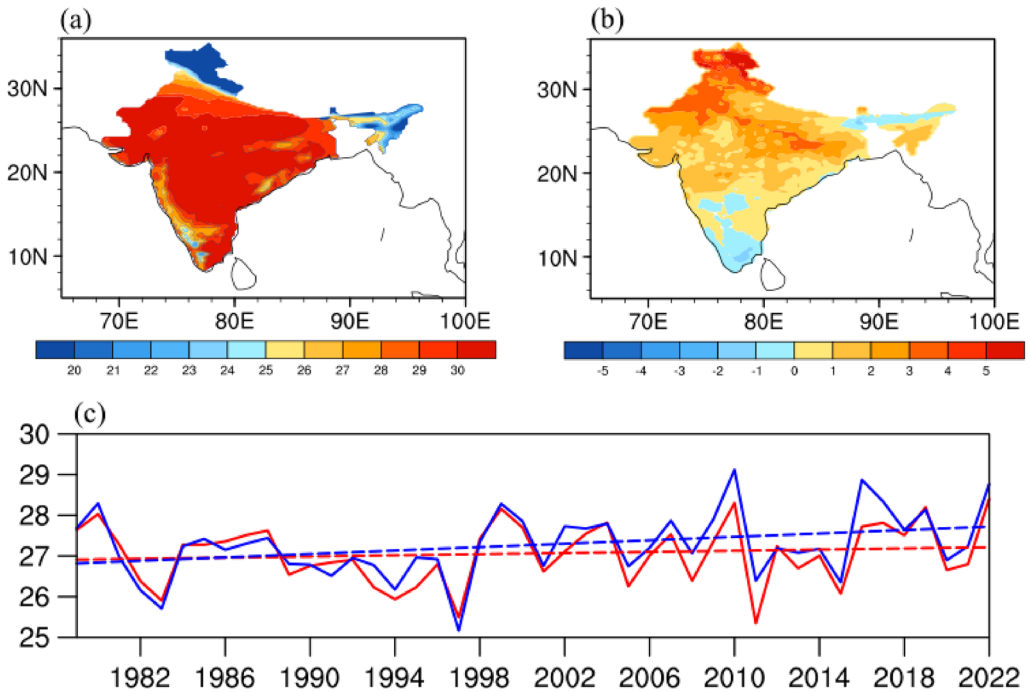

Fig. 1 **a** The climatological mean of surface air temperature (SAT; °C) over the Indian continent during April for the period of 1979–2022. **b** The SAT anomalies over the Indian continent during April 2022. **c** The SAT averaged in the Indian continent (the SATI; solid lines) companied with the trend (dashed lines), obtained from NCEP (red) and ERA5 (blue)

the NCEP–NCAR. The former is more close to the trend obtained from the India Meteorological Department daily gridded station data (Sanjay et al. 2020). It is checked that the results of interannual variability are independent with different reanalysis, so that only results from ERA5 are shown. We calculated the monthly anomalies by subtracting the climatological mean annual cycle from the time series, and the trend is not removed in this study. The study period is from January 1979 to April 2022.

The ENSO indices (including Niño 1 + 2, Niño 3, Niño 3.4 and Niño 4) are download from https://psl.noaa.gov/data/climateindices/list/. The statistical significance of the correlation coefficient is tested with the Student's *t*-test, which determines whether two populations express a significant difference between the population means.

Results

The EOF analysis is applied to discover the spatial and temporal characteristics of SAT anomalies over the Indian continent. As shown in Fig. 2, the first two leading EOF modes of monthly SAT anomalies for the period 1979–2022 explain 44.0% and 13.9% of the total squared covariance, respectively. The EOF1 captures the same sign SAT anomalies over the whole of India. The first principal component (PC1) have an increasing trend, and

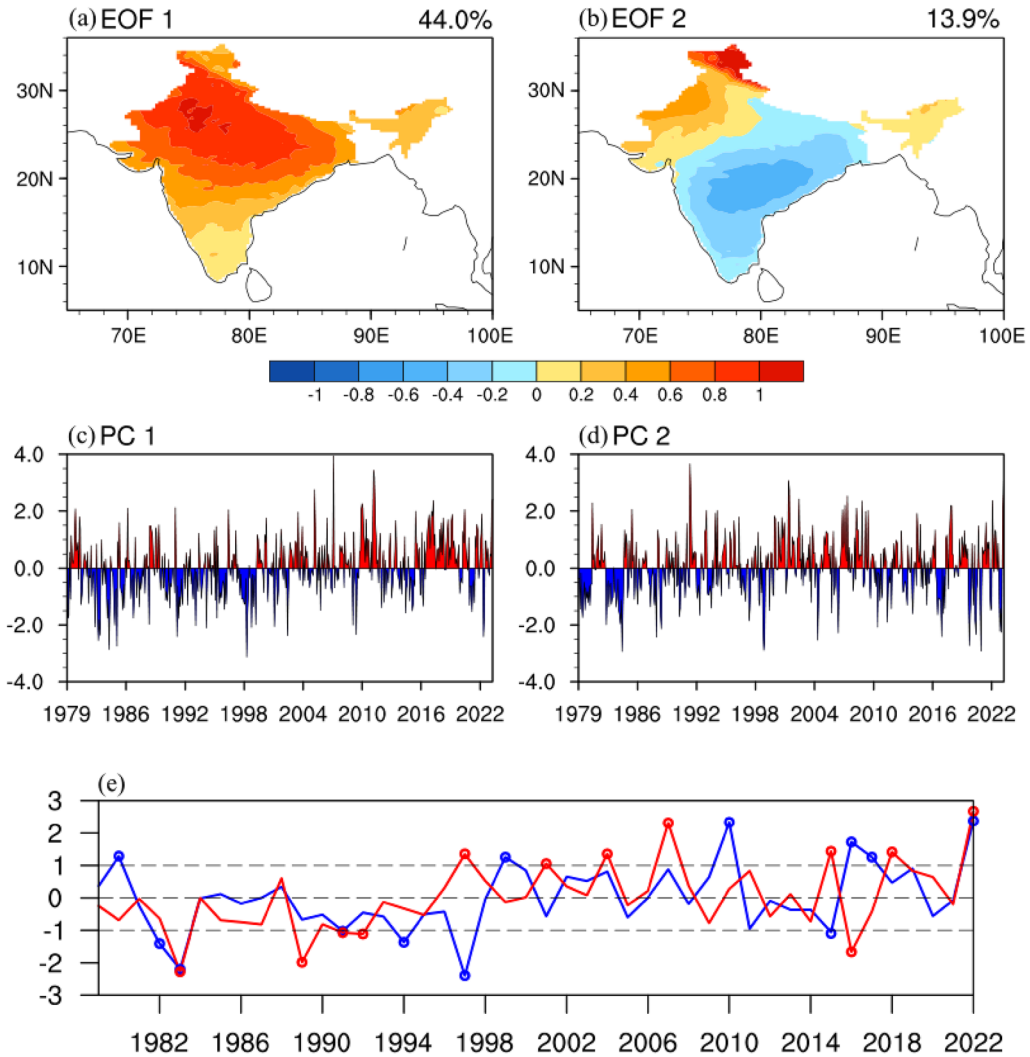

Fig. 2 Spatial patterns of **a** EOF1 and **b** EOF2 of the monthly SAT anomalies (°C) over Indian continent for the period of 1979–2022 (after removing the monthly mean regional average SAT). **c** and **d** Are the normalized time series of PCs. **e** The normalized time series of PC1 (red line) and PC2 (blue line) during April from 1979 to 2022. The pronounced EOFs cases are labeled with circles

it has a high correlation with the SATI (R = 0.99). In contrast, the EOF2 represents a "sea-saw" SAT anomaly pattern in the northwest–southeast direction. Similar results can also be obtained when applying the EOF analysis to the April SAT anomalies (not shown). These results are consistent with Chowdary et al. (2014) using air-temperature data from the University of Delaware for the period 1900–2005.

The spatial structures of EOF1 and EOF2 show a center of SAT anomaly over the northwestern India (Fig. 2a, b). Pattern correlations are employed to explore the linear relation between two spatial patterns. The pattern correlations between EOFs and SAT anomaly during April 2022 (Fig. 1b) can reach 0.90 (significant at the 99% confidence level). Thus, we assume that both the EOF1 and EOF2 have contributed to the extreme SAT anomaly over the northwestern India, although the EOFs are commonly orthogonal. The EOFs cases are further selected to prove this assumption. The positive (negative) EOFs cases are defined as the PCs during April that are larger than one standard deviation (smaller than minus one standard deviation), respectively. There are 6 (6) positive (negative) EOF1 cases and 7 (5) positive (negative) EOF2 cases from 1979 to 2022 (circles in Fig. 2e). One can see that the positive EOF1 and EOF2 cases only occur simultaneously during 2022. The PCs are higher than 2 during 2022, which results in the extreme warming over the northwestern India. Thus, the question that will be addressed in this study is—what controls the first two leading EOF modes and facilitates energizing them during 2022?

Figure 3a shows the regressions of the PC1 with SAT and sea level pressure anomalies during April from 1979 to 2022. Similar to Fig. 1b, the maximum of SAT anomalies occurs over the northwestern India and surrounding countries. Due to the surface warming, the sea level pressure anomalies decrease over the whole of Indian continent. According to the thermodynamic energy equation, the horizontal advection and diabatic heating related to short wave radiation are two main factors for the interannual variability of SAT. For the horizontal advection, the warm SST anomalies can be clearly seen in the Arabian Sea and Bay of Bengal, accompanied by anticlockwise surface wind anomalies (Fig. 3b). Such anomalous winds are favorable for the warm advection from the ocean surface to land in the boundary layer. Concurrently, surface net shortwave radiation also plays an important role in the SAT variability. As shown in Fig. 3c, d, an anomalous anti-cyclone appears in the troposphere, leading to the generation of deep convection and local downdraft. The latter reduces specific humidity anomaly in the low-level troposphere over India (Fig. 3c), leading to the decrease of clouds cover. As a result, shortwave radiation is enhanced at the surface, which thereby causes warming over the northwestern India. Overall, both the Indian Ocean warming and the atmospheric forcing are important reasons for the increase of Indian SAT.

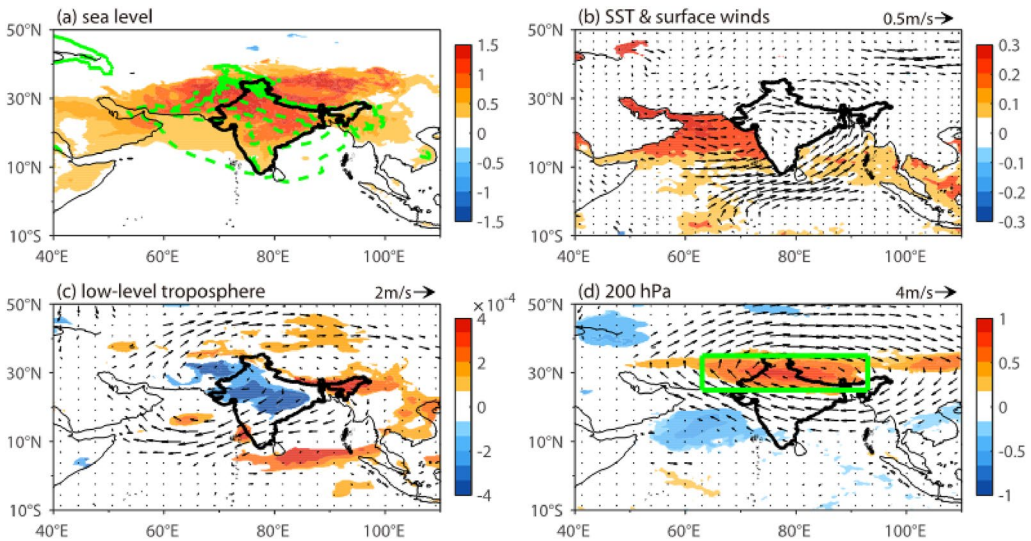

Fig. 3 Regressions of the PC1 with **a** SAT (colors; °C), sea level pressure (contours; hPa), **b** sea surface temperature (SST; colors; °C) and surface winds (vectors; m/s) for the period of 1979–2022. **c** Is the same as **b**, but for winds (vectors; m/s) at 700 hPa and the specific humidity (colors; g kg^{-1}) integral from 850 to 700 hPa. **d** Is the same as **b**, but for the vorticity (colors; × 10^5 s^{-1}) and winds (vectors; m/s) at 200 hPa. The green box marks the region from 25°N to 35°N and from 63°E to 93°E, which is used to define the anti-cyclone index (ACI). Only anomalies which are significant at 95% significance level are shown

Furthermore, the ocean warming is closely related to the Indian Ocean Basin Mode (IOBM), which is known as the first leading EOF mode of SST anomalies in the Indian Ocean (Klein et al. 1999; Alexander et al. 2002; Du et al. 2009; Schott et al. 2009). Although the IOBM is forced by ENSO-induced heat flux anomalies (Klein et al. 1999), the PC1 has low correlations with different ENSO indices (including Niño 1+2, Niño 3, Niño 3.4 and Niño 4), and all of which are below 0.1 (not significant at the 90% confidence level). The spatial pattern of IOBM from 1979 to 2022 is shown in Fig. 4a. The positive IOBM contains warm SST anomalies in the whole of Indian Ocean with the maximum in the equator. After the late 1970s, the center of action in the IOBM shifted towards the Arabian Sea (Sun et al. 2019), where the positive SST anomalies associated with the Indian warming are relatively large (Fig. 3b). The corresponding PC represents the temporal variability of IOBM, which is referred as to the IOBM index (IOBMI). The IOBMI has an increasing trend in recent years due to global warming (Zheng et al. 2011), and it has a close relationship with the SAT anomalies over India. As shown in Fig. 4b, the significant correlation coefficient occurs when the IOBMI leads the PC1 by 3 months (R=0.43), and reaches the highest with 2 months lead (R=0.45). The IOBM is energetic during boreal winter, and the SST anomalies can persist until summer (Fig. 4c; Yang et al. 2007). Due to the seasonal transition and SST forcing, the surface winds have shifted from northerly to westerly over the Arabian Sea, and from easterly to southerly over the Bay of Bengal. The SST anomalies and wind shift enhance warm advection from Indian Ocean to the land, which ultimately leads to the increase in SAT over India.

The results shown above reveal the capability of the IOBM and tropospheric anomalous anti-cyclone to influence the regional mean SAT during April. The strength of anomalous anti-cyclone is qualified by the vorticity anomaly at 200 hPa averaged in India (25 °–40 °N, 60 °–90 °E, where the vorticity anomaly is relatively large; green box in Fig. 3d), which is referred to as the AC index (ACI). The ACI has a high correlation with the SATI (R=0.6, significant at the 99% confidence level). In addition, the correlation coefficient between the IOBMI and ACI is relatively weak (R=− 0.09, not significant at the 90% confidence level), which suggests that the IOBM and the anomalous anti-cyclone are relatively independent of each other. Considering their tight relationship in predicting regional mean SAT over India, an empirical model is established to

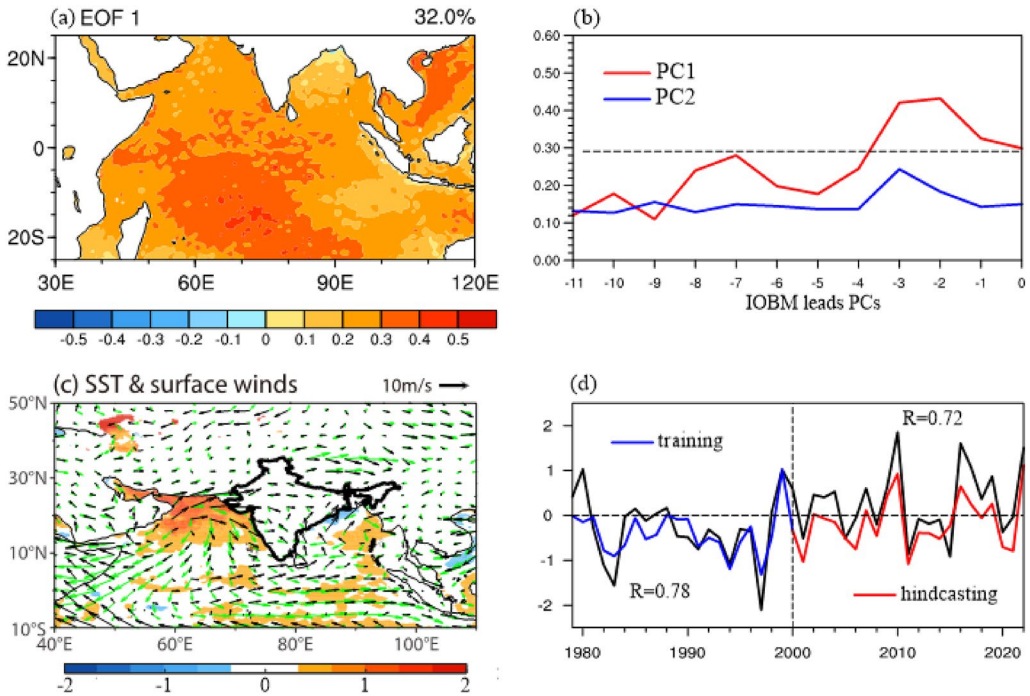

Fig. 4 **a** The spatial structure of the IOBM for the period of 1979–2022, calculated by the EOF function of monthly SST anomalies obtained from ERSST. **b** The lead correlation coefficient of the monthly IOBMI with the April PC1 (red line) and PC2 (blue line) during the period of 1979–2022. The zero of x-axis represents the concurrent correlation. **c** Regression of April SST anomalies with the January IOBMI (colors; °C). The green and black vectors are the mean surface winds during March and April (m/s). **d** The normalized SATI (black line; the same as the blue line in Fig. 1c), the predicted SATI for the training period (blue line; 1979–2000) and the hindcasting period (red line; 2000–2022)

predict the Indian SAT during April (referred to as the predicted SATI) based on both the IOBMI and the ACI:

$$Predicted\ SATI_{April} = \alpha \cdot IOBMI_{January} + \beta \cdot ACI_{April}.$$

Since the significant correlation occurs when the IOBMI leads the SATI around 3 months, the January IOBMI is chosen (Fig. 4b). The training time window is chosen from 1979 to 2000, and the half period 2000–2022 of time is used for hindcasting period. Statistically, the comparable time length during two periods provides the guarantee for the comparison of the prediction performance, which is quantified by the correlation coefficient. The parameters $\alpha = 0.14$ and $\beta = 0.59$ are calculated by a least-squares fit to the IOBMI and the ACI, respectively. To assess the prediction skills of this model, we compare the predicted SATI with observations (Fig. 4d). There is a high correlation coefficient (R = 0.72) between the observed SATI and that predicted by the above model. It indicates that the IOBM and the anomalous anti-cyclone are essential factors of regional mean SAT over India, which are beneficial to improve the prediction of Indian SAT during April. Additionally, although the anomalous anti-cyclone is not active during 2022 (the ACI is under one standard deviation), the intensified IOBM is strong enough to motivate warming over India (the IOBMI is higher than one standard deviation), which is reproduced by the predicted SATI (Fig. 4d).

However, the SAT anomaly pattern during April 2022 (Fig. 1b) cannot totally be explained by the EOF1, which represents the regional mean SAT over India. The extreme high temperature over the northwestern India is also linked to the EOF2 pattern. For the EOF2 pattern, the regression map has a marked wave train through North Atlantic and Europe (Fig. 5a). Such wave train leads to the high pressure at 200 hPa over the northern India, which is the dominant factor for the dipole pattern of Indian SAT anomalies during April (i.e., EOF2). The high pressure at 200 hPa is in favor of the downdraft to the north of India, leading to the increased short wave radiation in this region. As a result, the SAT anomalies are enhanced. To confirm this, we calculate the Rossby Wave Source (RWS; Sardeshmukh and Hoskins 1988) and Rossby wave rays (Hoskins and Ambrizzi 1993). As shown in Fig. 5b, a significant RWS center can be seen over the northwestern Atlantic (color shading). The Rossby wave rays originate from this RWS center with the climatological April 200 hPa zonal winds as basic flow, and the initial wavenumbers for the wave rays are chosen to be 1–3. Most branches of wave rays are characterized by clear eastward propagation from the northwestern Atlantic to the continent of Europe, which is in agreement with the spatial scale of the observed wave train (Fig. 5a).

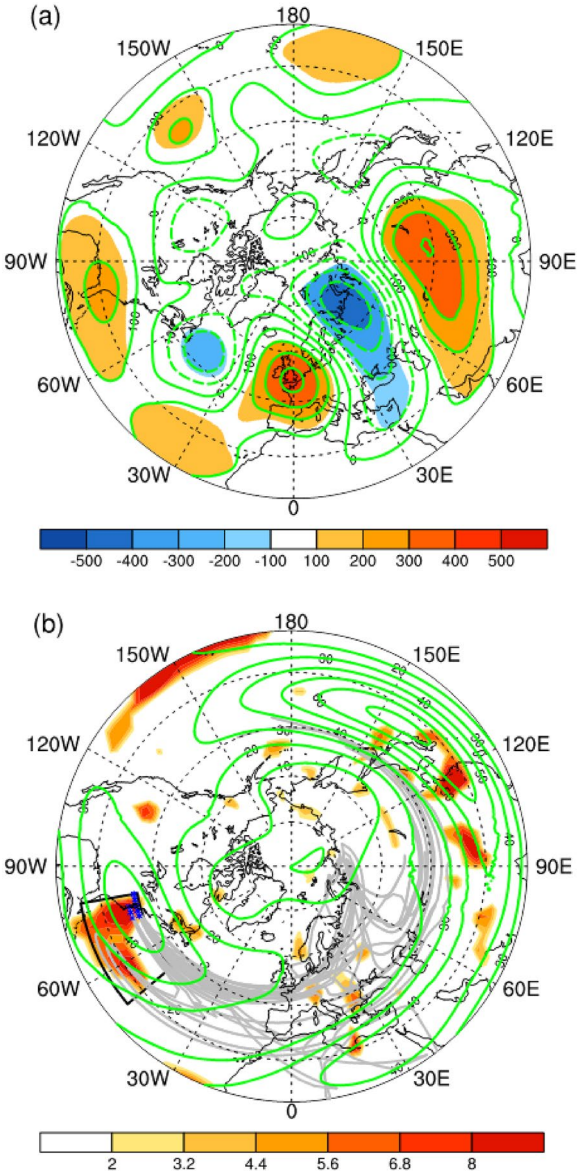

Fig. 5 Regression of the PC2 with **a** geopotential height at 200 hPa (contours; m) and **b** Rossby wave source (s^{-2}) during April from 1979 to 2022. The significant results are marked in **a**. The green contours in **b** represent the mean zonal winds at 200 hPa during April from 1979 to 2022, and the gray contours are Rossby wave trajectories along the wave pathways (the initial positions are marked). The black box marks the region from 25°N to 40°N and from 80°W to 50°W

We further check that the SST anomalies have non-significant correlations with the PC2, which indicates the role of atmospheric forcing in the Rossby waves. The center of RWS anomaly over the Northwestern Atlantic (25 °–40 °N, 50 °–80 °W; black box in Fig. 5b) has a high correlation with PC2 (R = 0.58, significant at the

95% confidence level), and it is higher than 15 s^{-2} during April 2022, which strengths the Rossby wave train and anomalous anti-cyclone over the northern India. Hence, it provides a basic guarantee of the occurrence of extreme SAT during April 2022.

Conclusion and discussion

Besides the influence of global warming on the trend of Indian SAT discussed in most previous studies, the Indian SAT has a non-negligible interannual variability, which is an important reason for the extreme heat wave events over India. In this study, we examined the mechanism for the interannual variability of Indian SAT during April and the reasons for the high record SAT during April 2022. The EOF results show that the first two leading modes of Indian SAT anomalies are concurrently active during April 2022. The EOF1 is forced by the IOBM and the anomalous deep anti-cyclone in the troposphere. The former is pronounced during 2022, strengthening the warm advection from ocean to land and intensifying warming over the whole of India. The EOF2 is associated with the Rossby wave train from Northwestern Atlantic to the north of India, which is the other cause for the unprecedented warming over northwestern India during April 2022. Moreover, we reconstruct the regional mean SAT over India using the IOBMI and the vorticity anomalies associated with the tropospheric anti-cyclone, indicating their ability to improve prediction skills for the SAT over India.

Some studies suggested the remote impact of ENSO in the variability of Indian SAT (e.g., Chowdary et al. 2014) and the ENSO benefits for the prediction on seasonal to interdecadal timescales (e.g., Hou et al. 2022). However, we find that the local forcing is more important to the interannual variability of Indian SAT. The SATI has low correlations with different ENSO indices (below 0.1), and the peaks of PCs do not always occur after the ENSO years (e.g., 1982, 1997, 2010; Fig. 2e). Although the IOBM is a consequence of ENSO (Klein et al. 1999; Alexander et al. 2002; Du et al. 2009; Schott et al. 2009), rich upper ocean processes in the tropical Indian Ocean, including horizontal and vertical advection, overturning and turbulent mixing (Shenoi et al. 2002; Shee et al. 2019; Jain et al. 2021; Qin et al. 2022), also play important roles in the SST change on multi-scales. Numerical experiments are needed to further qualify the impacts of atmospheric and oceanic forcing on the SST variation, which triggers the increase of Indian SAT.

Our results shed light on the atmospheric physical processes that translate Rossby wave train to the SAT interannual variability over India, and provide a clear way forward to predict the Indian SAT. It is reported by Kornhuber et al. (2020) that Rossby waves are associated with a strongly meandering jet stream and might cause simultaneous heatwaves across the northern hemisphere. On the decadal timescale, the presence of an upper-level cyclonic anomaly over the west of North Africa has an impact on the increase in the number of intensive heat waves (Rohini et al. 2016). Thus, atmospheric teleconnections should focus on the studies of global and regional extreme SAT in the current climate.

Acknowledgements

Not applicable

Author contributions

JQ performed the data analyses and wrote the manuscript; HL helped perform the analysis with constructive discussions; BL contributed significantly to the improvement of the manuscript. All authors read and approved the final manuscript.

Funding

This work is supported by grants from the National Natural Science Foundation of China (42106003), the China Postdoctoral Science Foundation (2022M711010), and the Fundamental Research Funds for the Central Universities (B210202142).

Availability of data and materials

All observation data and reanalysis products for this paper are properly cited and referred to in the reference list. ERA5 reanalysis are available at https://www.ecmwf.int/en/forecasts/datasets/reanalysis-datasets/era5. ERSST and NCEP-NCAR reanalysis are publicly available from the National Oceanic and Atmospheric Administration (https://psl.noaa.gov/data/gridded/data.noaa.ersst.v5.html, https://www.esrl.noaa.gov/psd/data/gridded/data.ncep.reanalysis.html).

Declarations

Competing interests

The authors declare no competing financial or non-financial interests.

Received: 5 October 2022 Accepted: 18 December 2022
Published online: 05 January 2023

References

Alexander MA, Bladé I, Newman M, Lanzante JR, Lau NC, Scott JD (2002) The atmospheric bridge: The influence of ENSO teleconnections on air–sea interaction over the global oceans. J Clim 15(16):2205–2231. https://doi.org/10.1175/1520-0442(2002)015%3c2205:TABTIO%3e2.0.CO;2

Bjerknes J (1969) Atmospheric teleconnections from the equatorial pacific. Mon Weather Rev 97(3):163–172. https://doi.org/10.1175/1520-0493(1969)097%3c0163:ATFTEP%3e2.3.CO;2

Blunden J, Hartfield G, Arndt DS, Dunn R, Tye M, Blenkinsop S, Jacobs S (2018) State of the Climate in 2017. Bull Am Meteorol Soc 99(8):Si-S310. https://doi.org/10.1175/2019BAMSStateoftheClimate.1

Chowdary JS, John N, Gnanaseelan C (2014) Interannual variability of surface air-temperature over India: impact of ENSO and Indian Ocean Sea surface temperature. Int J Climatol 34(2):416–429. https://doi.org/10.1002/joc.3695

De US, Dube RK, Rao GP (2005) Extreme weather events over India in the last 100 years. J. Ind. Geophys. Union, 9(3):173–187. http://sa.indiaenvironmentportal.org.in/files/extreme%20events.pdf

Du Y, Xie SP, Huang G, Hu K (2009) Role of air–sea interaction in the long persistence of El Niño-induced north Indian Ocean warming. J Clim 22(8):2023–2038. https://doi.org/10.1175/2008JCLI2590.1

Hersbach H, Bell B, Berrisford P, Horányi A, Sabater JM, Nicolas J et al (2019) Global reanalysis: goodbye ERA-Interim, hello ERA5. ECMWF Newsl 159:17–24. https://doi.org/10.21957/vf291hehd7
Hingane LS, Rupa Kumar K, Ramana Murthy BHV (1985) Long-term trends of surface air temperature in India. Int J Climatol 5:521–528. https://doi.org/10.1002/joc.3370050505
Hoskins BJ, Ambrizzi T (1993) Rossby wave propagation on a realistic longitudinally varying flow. J Atmos Sci 50(12):1661–1671. https://doi.org/10.1175/1520-0469(1993)050%3c1661:RWPOAR%3e2.0.CO;2
Hou Z, Li J, Ding R, Feng J (2022) Investigating decadal variations of the seasonal predictability limit of sea surface temperature in the tropical Pacific. Clim Dyn. https://doi.org/10.1007/s00382-022-06179-3
Jain V, Shankar D, Vinayachandran PN, Mukherjee A, Amol P (2021) Role of ocean dynamics in the evolution of mixed-layer temperature in the Bay of Bengal during the summer monsoon. Ocean Model 168:101895. https://doi.org/10.1016/j.ocemod.2021.101895
Kalnay E, Kanamitsu M, Kistler R, Collins W, Deaven D, Gandin L et al (1996) The NCEP/NCAR 40-year reanalysis project. Bull Am Meteor Soc 77(3):437–472. https://doi.org/10.1175/1520-0477(1996)077%3c0437:TNYRP%3e2.0.CO;2
Kalsi SR, Pareek RS (2001) Hottest April of the 20th century over north-west and central India. Current science, 867–873. http://www.jstor.org/stable/24105739
Klein SA, Soden BJ, Lau NC (1999) Remote sea surface temperature variations during ENSO: evidence for a tropical atmospheric bridge. J Clim 12(4):917–932. https://doi.org/10.1175/1520-0442(1999)012%3c0917:RSSTVD%3e2.0.CO;2
Kornhuber K, Coumou D, Vogel E, Lesk C, Donges JF, Lehmann J, Horton RM (2020) Amplified Rossby waves enhance risk of concurrent heatwaves in major breadbasket regions. Nat Clim Chang 10(1):48–53. https://doi.org/10.1038/s41558-019-0637-z
Kothawale DR, Rupa Kumar K (2005) On the recent changes in surface temperature trends over India. Geophys Res Lett. https://doi.org/10.1029/2005GL023528
Krishnan R, Sabin TP, Vellore R, Mujumdar M, Sanjay J, Goswami BN, Terray P (2016) Deciphering the desiccation trend of the South Asian monsoon hydroclimate in a warming world. Clim Dyn 47(3):1007–1027. https://doi.org/10.1007/s00382-015-2886-5
Kumar KR, Kumar KK, Pant GB (1994) Diurnal asymmetry of surface temperature trends over India. Geophys Res Lett 21(8):677–680. https://doi.org/10.1029/94GL00007
Pai DS, Srivastava AK, Nair SA (2017) Heat and cold waves over India. In Observed climate variability and change over the Indian Region. Springer, Singapore, pp 51–71. https://doi.org/10.1007/978-981-10-2531-0_4
Qin J, Meng Z, Xu W, Li B, Cheng X, Murtugudde R (2022) Modulation of the intraseasonal chlorophyll-a concentration in the tropical Indian Ocean by the central Indian Ocean mode. Geophys Res Lett. https://doi.org/10.1029/2022gl097802
Rai A, Joshi MK, Pandey AC (2012) Variations in diurnal temperature range over India: under global warming scenario. J Geophys Res Atmos. https://doi.org/10.1029/2011JD016697
Rohini P, Rajeevan M, Srivastava AK (2016) On the variability and increasing trends of heat waves over India. Sci Rep 6(1):1–9. https://doi.org/10.1038/srep26153
Ross RS, Krishnamurti TN, Pattnaik S, Pai DS (2018) Decadal surface temperature trends in India based on a new high-resolution data set. Sci Rep 8(1):1–10. https://doi.org/10.1038/s41598-018-25347-2
Roy SS, Balling RC Jr (2005) Analysis of trends in maximum and minimum temperature diurnal temperature range, and cloud cover over India. Geophys Res Lett. https://doi.org/10.1029/2004GL022201
Sanjay J, Revadekar JV, Ramarao MVS, Borgaonkar H, Sengupta S, Kothawale DR, Ratnam JV (2020) Temperature changes in India. in assessment of climate change over the Indian region. Springer, Singapore, pp 21–45. https://doi.org/10.1007/978-981-15-4327-2_2
Sardeshmukh PD, Hoskins BJ (1988) The generation of global rotational flow by steady idealized tropical divergence. J Atmos Sci 45(7):1228–1251. https://doi.org/10.1175/1520-0469(1988)045%3c1228:TGOGRF%3e2.0.CO;2
Schott FA, Xie SP, McCreary JP Jr (2009) Indian Ocean circulation and climate variability. Rev Geophys. https://doi.org/10.1029/2007RG000245
Shee A, Sil S, Gangopadhyay A, Gawarkiewicz G, Ravichandran M (2019) Seasonal evolution of oceanic upper layer processes in the Northern Bay of Bengal following a single Argo float. Geophys Res Lett 46(10):5369–5377. https://doi.org/10.1029/2019GL082078
Shenoi SSC, Shankar D, Shetye SR (2002) Differences in heat budgets of the near-surface Arabian Sea and Bay of Bengal: Implications for the summer monsoon. J Geophys Res Oceans 107(C6):5–1. https://doi.org/10.1029/2000JC000679
Sun B, Li H, Zhou B (2019) Interdecadal variation of Indian Ocean basin mode and the impact on Asian summer climate. Geophys Res Lett 46(21):12388–12397. https://doi.org/10.1029/2019GL085019
Yang J, Liu Q, Xie SP, Liu Z, Wu L (2007) Impact of the Indian Ocean SST basin mode on the Asian summer monsoon. Geophys Res Lett. https://doi.org/10.1029/2006GL028571
Zheng XT, Xie SP, Liu Q (2011) Response of the Indian Ocean basin mode and its capacitor effect to global warming. J Clim 24(23):6146–6164. https://doi.org/10.1175/2011JCLI4169.1

Publisher's Note